TECHNICAL REVIEW

No. 1 – 2010

Time Selective Response Method
In situ Measurement of Absorption Coefficient
Transverse Motion in Accelerometer Calibration

Courtesy of Dassault Aviation

www.bksv.com

Brüel & Kjær

creating sustainable value

Previously issued numbers of Brüel & Kjær Technical Review

(Continued from cover page 2)

1 – 1997 A New Design Principle for Triaxial Piezoelectric Accelerometers
A Simple QC Test for Knock Sensors
Torsional Operational Deflection Shapes (TODS) Measurements
2 – 1996 Non-stationary Signal Analysis using Wavelet Transform, Short-time Fourier Transform and Wigner-Ville Distribution
1 – 1996 Calibration Uncertainties & Distortion of Microphones.
Wide Band Intensity Probe. Accelerometer Mounted Resonance Test
2 – 1995 Order Tracking Analysis
1 – 1995 Use of Spatial Transformation of Sound Fields (STSF) Techniques in the Automative Industry
2 – 1994 The use of Impulse Response Function for Modal Parameter Estimation
Complex Modulus and Damping Measurements using Resonant and Non-resonant Methods (Damping Part II)
1 – 1994 Digital Filter Techniques vs. FFT Techniques for Damping Measurements (Damping Part I)
2 – 1990 Optical Filters and their Use with the Type 1302 & Type 1306 Photoacoustic Gas Monitors
1 – 1990 The Brüel & Kjær Photoacoustic Transducer System and its Physical Properties
2 – 1989 STSF – Practical Instrumentation and Application
Digital Filter Analysis: Real-time and Non Real-time Performance
1 – 1989 STSF – A Unique Technique for Scan Based Near-Field Acoustic Holography Without Restrictions on Coherence
2 – 1988 Quantifying Draught Risk
1 – 1988 Using Experimental Modal Analysis to Simulate Structural Dynamic Modifications
Use of Operational Deflection Shapes for Noise Control of Discrete Tones

Special technical literature

Brüel & Kjær publishes a variety of technical literature which can be obtained from your local Brüel & Kjær representative.

The following literature is presently available:

- Catalogues (several languages)
- Product Data Sheets (English, German, French,)

Furthermore, back copies of the Technical Review can be supplied as listed above. Older issues may be obtained provided they are still in stock.

Technical Review

No. 1 – 2010

Contents

Editor: Harry K. Zaveri

Time Selective Response Measurements – Good Practices and Uncertainty*

Erling Sandermann Olsen and Rémi Guastavino

Abstract

Time Selective Response, TSR, is a frequency response measurement method based on linearly swept sine signals. Because TSR can be used for free-field measurements in ordinary rooms and is fast, accurate and relatively insensitive to background noise, it is convenient for measurements of microphone and sound level meter free-field responses. However, the method's combination of time and frequency weighting can make it complicated to estimate the uncertainty of the measured response. This paper briefly summarizes the method and presents some experience with and guidelines for choosing measurement and weighting parameters and considerations on the associated uncertainty on the results. The results are discussed on the basis of practical measurements of microphone and sound level meter free-field responses at Brüel & Kjær.

Résumé

Une mesure de réponse en fréquence par la méthode TSR (Time Selective Response) fait intervenir un balayage linéaire de signaux sinusoïdaux. Cette méthode utilisable dans les pièces ordinaires pour des mesures en champ libre, rapide et précise, relativement peu sensible au bruit de fond, est pratique pour les mesures de réponse en fréquence en champ libre des microphones et des sonomètres. Toutefois, l'application d'une combinaison des pondérations temporelle et fréquentielle complique quelque peu l'estimation de l'incertitude sur la réponse mesurée. Ces pages résument la méthode et font part de considérations pratiques sur le choix des paramètres de mesurage et de pondération ainsi que sur l'incertitude que ce paramétrage induit sur les résultats. Ces résultats sont discutés sur la base de mesurages de réponse de fréquence en champ libre de microphones et sonomètres réalisés à l'usine Brüel & Kjaer.

* First published at INTER-NOISE 2010, Lisbon, Portugal

Zusammenfassung

Time Selective Response (TSR) ist eine Methode zur Frequenzgangmessung, die auf linearer Gleitsinusanregung beruht. TSR ermöglicht Freifeldmessungen in normalen Räumen und ist schnell, präzise und relativ unempfindlich gegenüber Störgeräuschen. Damit empfiehlt sich die Methode für die Messung der Freifeldfrequenzgänge von Mikrofonen und Schallpegelmessern. Die verwendete Kombination von Zeit- und Frequenzbewertung kann jedoch die Unsicherheitsbestimmung des gemessenen Frequenzgangs komplizieren. Neben einer kurzen Beschreibung der Methode präsentiert der Artikel Erfahrungen und Hinweise in Verbindung mit der Auswahl von Mess- und Bewertungsparametern, sowie Betrachtungen über die durch sie bedingte Unsicherheit der Ergebnisse. Die Ergebnisse werden anhand praktischer Messungen der Freifeldfrequenzgänge von Mikrofonen und Schallpegelmessern bei Brüel & Kjær diskutiert.

Introduction

In 1991, Brüel & Kjær introduced Audio Analyzer Type 2012 with its Time Selective Response (TSR) measuring algorithm. With the TSR method, the system responses of electroacoustic devices can be measured reliably in ordinary rooms. Type 2012 is not produced anymore, but since the release of the PULSE™ 12 Multi-analyzer Platform, TSR has also been available on Brüel & Kjær's present family of sound and vibration analyzers.

The TSR method provides a fast and convenient way to perform free-field measurements in reflective environments, but the combination of time and frequency weighting in the method can make it complicated to estimate the uncertainty of the measured response.

This paper presents some guidelines for choosing measurement and weighting parameters and considerations on the associated uncertainty on the results.

TSR Method

Signal Processing of TSR

Time Selective Response, TSR, is a frequency response measurement method based on linearly swept sine signals. The method is based on Poletti's [1, 2] ideas that solved some issues that could lead to erroneous measurement in earlier methods. The method is based on an underlying assumption on linearity and

invariance of the object response. The impulse response of the system is determined by combining the inverted excitation signal with the response signal. Reflections can be excluded from the measurement by selecting the desired part of the impulse response by weighting with a time window.

The excitation signal in TSR is a complex, linear sweep:

$$s(t) = e^{j\pi kt^2} \tag{1}$$

The resulting output signal is:

$$y(t) = h(t)*s(t) = \int_{-\infty}^{\infty} h(\upsilon)e^{j\pi k(t-\upsilon)^2}d\upsilon \tag{2}$$

where $h(t)$ is the impulse response of the object response, the transfer function of the complete measurement setup and the surrounding room. In the analysis, the output signal is combined with the inverse sweep:

$$\begin{aligned} u(t) &= e^{-j\pi kt^2}y(t) \\ &= e^{-j\pi kt^2}\int_{-\infty}^{\infty} h(\upsilon)e^{j\pi k(t-\upsilon)^2}d\upsilon \\ &= e^{-j\pi kt^2}\int_{-\infty}^{\infty} h(\upsilon)e^{j\pi k(t^2+\upsilon^2-2t\upsilon)}d\upsilon \\ &= \int_{-\infty}^{\infty}\left[h(\upsilon)e^{j\pi k\upsilon^2}\right]e^{-j2\pi kt\upsilon}d\upsilon \end{aligned} \tag{3}$$

Inserting $\xi = kt$, this has the form:

$$u(\xi) = \int_{-\infty}^{\infty}\left[h(\upsilon)e^{j\pi k\upsilon^2}\right]e^{-j2\pi\xi\upsilon}d\upsilon \tag{4}$$

The integral is recognised as the Fourier transform of the product of the system impulse response and the linear sweep, $h(t)e^{j\pi kt^2}$. Hence, using the convolution theorem:

$$\begin{aligned} h(t) &= e^{-j\pi kt^2} F^{-1}\{u(\xi)\} \\ &= e^{-j\pi kt^2} \int_{-\infty}^{\infty} u(\xi) e^{j2\pi\xi t} d\xi \end{aligned} \tag{5}$$

From this it is seen that $h(t)$ can be calculated for any point in time from the complete response. In particular, the time range including the direct sound from the measurement object can be selected for further calculation. The frequency response function can then be calculated by Fourier transform of $h(t)$:

$$H(f) = F\{h(t)\} \tag{6}$$

Conceptually, TSR can be understood as a combination of the swept sine signal and a tracking filter that follows the signal with a delay so that only the frequencies arriving at a certain delay are included in the measurement. The tracking filter is equivalent to the weighting function that defines the selected time range (Fig. 1).

The TSR algorithm effectively works as a zoom FFT around the centre of the swept frequency range, i.e., the impulse response that is determined is frequency shifted to the centre frequency of the sweep. This property means that the sweep does not need to cover the full frequency range of the target transfer function.

The TSR method requires measurement of the complex response function. If the measured frequency range is limited so that negative frequencies are not included in the full sweep, the complete function can be calculated from a single sine sweep, but if the sweep includes zero or negative frequencies, a cosine and subsequently a sine sweep must be made in order to obtain the complex function.

Windows in TSR

In addition to the time window that is (or can be) deliberately applied to the time response in a TSR measurement, there are two window functions inherently applied to the signal.

Fig. 1. Illustration of the concept of a tracking filter, from [3, 4]

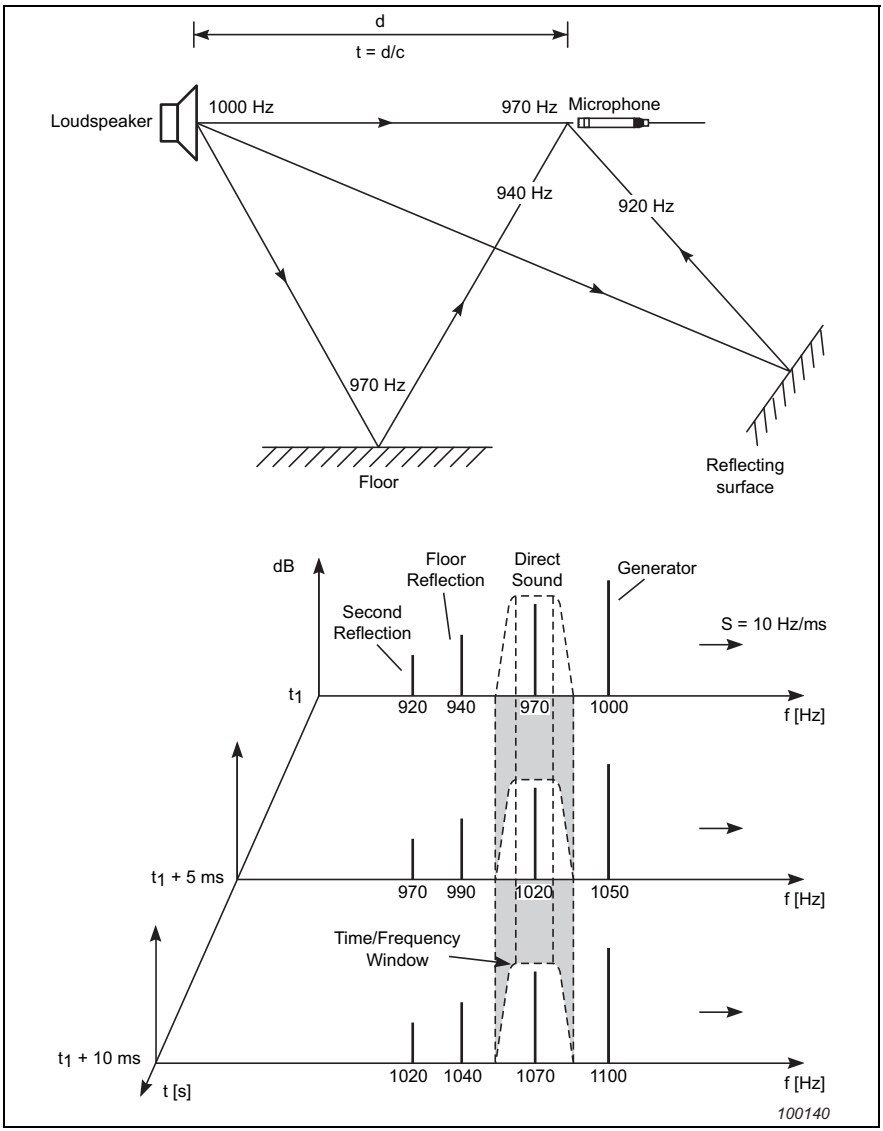

The first window inherent to the method is due to the limitation of the frequency sweep to the specified range. This is equivalent to applying a window function to an infinitely long frequency sweep:

$$s(t) = W_1(t)e^{j\pi kt^2} \tag{7}$$

The frequency spectrum of the finite sweep is determined by this weighting function.

The combination with the inverse (unweighted) sweep does not by itself distort the resulting impulse response.

The second window inherent to the method is due to the limitation of the analysis to a certain time range, and this is also effectively an application of a window to the impulse response, the time range mentioned above:

$$h(t) = W_2(t)e^{-j\pi kt^2} \int_{-\infty}^{\infty} u(\xi)e^{j2\pi\xi t}d\xi \tag{8}$$

The second window defines the time range that is included in the final Fourier transform so as to obtain the frequency response. Subsequent application of a narrower time window in order to exclude reflections is effectively the same as narrowing the time range, except that the time steps and frequency steps in the analysis are maintained.

The windows that are applied in Brüel & Kjær's TSR analyzers are Tukey windows, i.e., rectangular windows tapered with raised cosine functions. The user-selectable time window is a generalised form where the width of the two tapers can be selected independently.

In order to minimise the influence of the window applied to the sweep, the actual sweep covers a larger frequency range than that specified for the analysis.

The influence of the windows on the final result not only depends on the windows themselves, but is also a combination of the windows and the response to be measured. Therefore, it is not possible to predict the exact uncertainty based on the measurement parameters alone.

Applications of TSR

Since the TSR method provides time selectivity and both the time and frequency responses are immediately available, it is convenient for a large range of applications.

The method can be used for accurate and fast comparison calibration of microphones and sound level meters and measurement of the influence of accessories, etc. Due to the time selectivity, no anechoic chamber is needed for the measurements.

The method can be used for simple absolute frequency response measurements of, for example, loudspeakers. A procedure for combining far-field measurements with the TSR method with traditional near-field measurements for a loudspeaker is described in [5].

Another useful application of the TSR method is to use it as an effective means for localising reflections in a measured response. This can be used in optimising devices to disturb a sound field as little as possible. In particular this is relevant during the development of sound level meters, microphone holders, loudspeaker enclosures and similar devices.

Parameter Choice

Sweep Length

As can be seen from the expressions in “Signal Processing of TSR” on page 2, the sweep rate, and thus the sweep length, only influences the integration time, not the resolution of the measured impulse response. This means that the sweep length only influences the signal-to-noise ratio of the measurement. Some investigation should be done with the signal-to-noise ratio. If lowering the signal level by 10 dB significantly changes the measured response, the signal-to-noise ratio should be improved. If the noise itself cannot be reduced or the signal level increased, there are two ways to improve the signal-to-noise ratio in the TSR method. Either the sweep length or the number of averages must be increased. The sweep length does not have any other influence on the measurement result, provided that the underlying overall assumption on linearity and invariance of the system is fulfilled.

Frequency Range

The choice of frequency range in the measurement has only minor influence on the measurement. This is due to the fact that TSR effectively works as a zoom FFT

around the centre frequency of the sweep. The spectrum of the frequency sweep will be convolved with the object response, but if the weighting function that defines the sweep is reasonably designed, this will have insignificant influence on the valid (selected) frequency range. This is illustrated in Fig. 2. Note that the frequency range shown in the figure includes the part that is generated outside the specified frequency range so as to minimise the influence of the limitation of the sweep.

Fig. 2. Simulated absolute response measurement with different frequency ranges. The time window is the full time range of the analysis

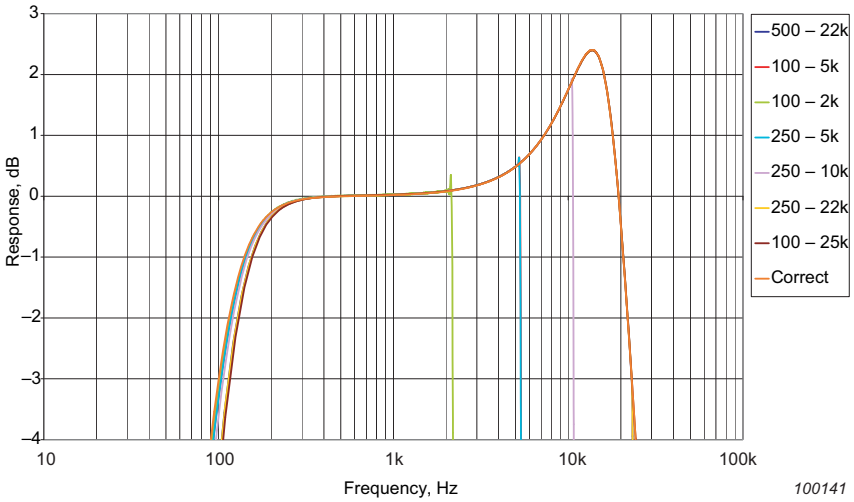

Time Window

The time window is a critical parameter in the TSR method (as in any other time selective method). Ideally, the time window should include the complete time response and exclude all other information.

In order to include all the desired information, the time window must at least be sufficiently long so as to include the fluctuations of the object response:

$$T_{\min} = 1/f_c \tag{9}$$

where f_c is the necessary frequency resolution. If the time window is too short, it will behave as a smoothing function on the response. This may be acceptable in

some cases at high frequencies, for example in relative measurements where the resolution is not required in the measured ratio, but if the object response rolls off at low frequencies, too short a time window may deteriorate a large part of the object response.

The geometry of the measurement setup should be considered carefully. Simple measurement of the size of the measurement object helps in determining the minimum time window, and geometrical consideration can also help in optimising the path length difference in the setup.

In a normal building, the open height below room lighting, etc., is typically around 2.5 m. With a measuring distance of 1 m to 2 m, this leaves a difference between the direct path and the first reflected path of 1.2 m to 1.7 m, corresponding to a time difference between the direct sound and the first reflection of 3.5 ms to 4.9 ms. This limits the low-frequency resolution that can be achieved in time selective measurements in normal-sized rooms. If a higher resolution is desired, a room must be used where the distance to any reflecting objects is larger. This may, however, require more bulky mounting devices that again may lead to less stable mounting and be more susceptible to the movement of air in the room. A time window allowing measurement of a 3.5 ms long time response will be sufficient for most applications within microphone and loudspeaker measurements.

It is important that the time window only covers the part of the object time response that contains significant energy. In other words, if the complete impulse response of the measurement object is included in the time window, no further information can be obtained with a longer time window, and the smoothing properties of the window do not deteriorate the object function. One important aspect of this is that the resolution of the result cannot be improved by extending the time window towards negative time from the impulse. This will only allow more noise to influence the measurement. This is illustrated in Fig. 3 (note, that the noise level is deliberately exaggerated in the example).

If it is possible within the limitations of the reflections, different measurement distances and time windows should be tried in order to resolve whether the complete impulse is included in the measurement. The necessary length of the time window can be determined experimentally by gradually increasing the length until the shape of the measured response does not change.

Fig. 3. Noise influence. Left: Time window covering the impulse response. Right: time window extended towards negative time

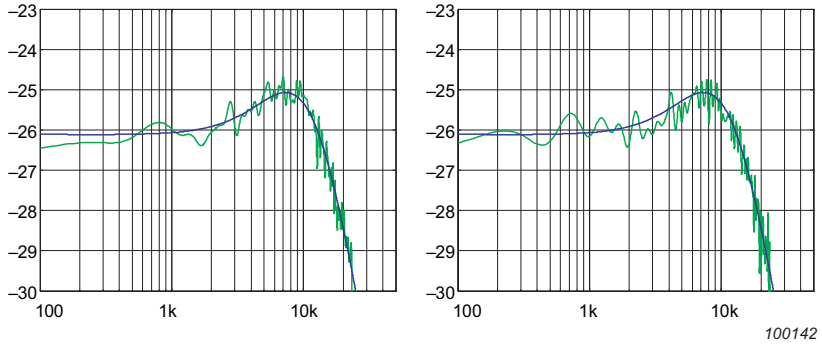

Uncertainty Estimation

Uncertainty estimation of frequency response measurements made with the TSR method is, of course, similar to that of any other frequency response measurement method, except for the aspects that are particular to the method. Here, the aspects related to TSR are discussed. Note, that these aspects are to some extent the same for other time selective methods, because the underlying principle of determining the impulse response and selecting a certain part is common to all these methods.

As mentioned and demonstrated, it is not possible to predict the exact uncertainty based on the measurement parameters alone. Some evaluation can be made on the maximum variation that can be anticipated, but that is likely to lead to overestimation of the uncertainty. Instead, the evaluation should be based on controlled variations or realistic modelling of the actual measurement situation.

In the case of the measurement of a single response, for example, in a loudspeaker measurement, the influence of the windows on the response contribute directly to the uncertainty of the measurement. If some knowledge is available of the object response, the influence of the parameters can be estimated by modelling. Alternatively, the measurement can be repeated with variations of the parameters. It should, however, be kept in mind that there may be systematic deviations that are not revealed by the possible parameter variations.

In the case of relative measurements where the response of the measurement object is compared with the response of a reference, for example, in microphone comparison calibration or measurement, some of the deviations due to the

windows cancel out because they are present in both measurements. In this case there are also considerable possibilities of making the measurements under different conditions both in the physical measurement setup and in the measurement parameters, thereby achieving knowledge on the uncertainty in the measurements.

In a frequency range where the reference and the object under test have similar and reasonably flat frequency responses, the low-frequency resolution does not hinder an accurate determination of the difference between the two, and the uncertainty on the determined frequency response can be relatively small if care is taken to avoid systematic errors.

Examples

In this section, a couple of examples of these measurements are used for illustration of the issues mentioned above. The TSR method is used extensively at Brüel & Kjær for measurements of free-field responses. It is the company's policy to thoroughly document all electroacoustic devices developed, and the TSR method has worked as an efficient and accurate tool for that purpose for several years.

Microphone Free-field Response Measurements

Free-field response measurements of microphones at Brüel & Kjær are exclusively made using the TSR method. Absolute free-field sensitivities are measured by comparison with reference microphones that are traceable to Danish national standards. Measurements of the influence of accessories such as wind screens, protection grids, etc., and directional characteristics are relative measurements where only the stability of the measurement object and the measurement setup is relevant. However, the measurements are always relative measurements. The free-field measurements with the TSR method are made at frequencies above 500 Hz. Below 500 Hz the free-field response of the microphones can reliably be established with other methods that are not the subject of this paper.

In order to ensure high accuracy and reproducibility in the measurements, some practices have been developed. Although these are not directly related to the TSR method, they are mentioned here in order to demonstrate how the TSR method is used.

Many of the measurements are carried out in a measurement room situated in a normal office building. Some factors such as circulating air, for example, due to ventilation systems, can disturb these measurements. Small pressure pulses are

generated in the building due to opening doors or the like and changing temperature causes changing speed of sound, detectable even when the changes are fractions of a degree. In order to minimise the variations in the measurement results due to these factors, the ventilation system is turned off during each response measurement that consists of six TSR sweeps. This can be done in a minimum of time. The six sweeps allows the identification of occasional (but rare) variations in the measurements as shown in Fig. 4. The practice also gives supplementary information to the uncertainty estimation.

Fig. 4. Variation of six consecutive sweeps. One of the sweeps has been disturbed

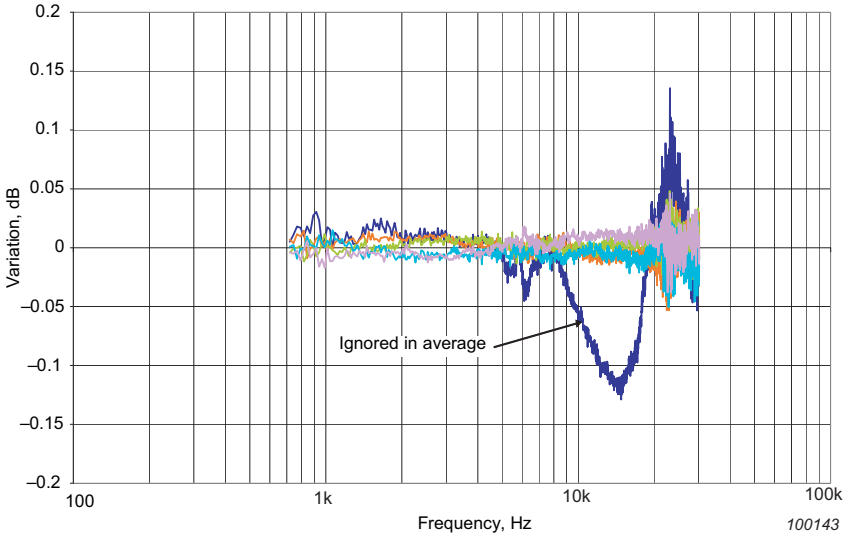

Sound Level Meter Free-field Response

The authors have recently worked with TSR measurements of sound level meter free-field frequency responses in order to establish well-documented uncertainty estimates on the free-field response of sound level meters.

Although the measurements in principle are similar to those of microphone free-field responses, the measurement of the free-field responses of large devices such as sound level meters and outdoor microphones is particularly challenging. The time window must be large in order not to exclude parts of the devices, and it is often difficult to mount the devices for measurement without having reflections from the mounting setup.

The authors' measurements are carried out in different rooms, with different loudspeakers, at different distances and with different frequency ranges. Fig. 5 shows the responses of the sound level meter and of the microphone on a long cylinder, and Fig. 6 shows the double standard deviation of the responses. As can be seen from the figures, it is indeed possible to achieve good reproducibility of these response measurements. Work is still going on to improve the measurement procedure and the data analysis, and has also been a part of the preparation of this paper.

Fig. 5. Measured free-field responses of a sound level meter and the sound level meter microphone carried out in widely different setups. Upper curves are for the microphone alone. Lower curves are for the microphone mounted on the sound level meter. The orange curve shows the low-frequency response in an enclosure

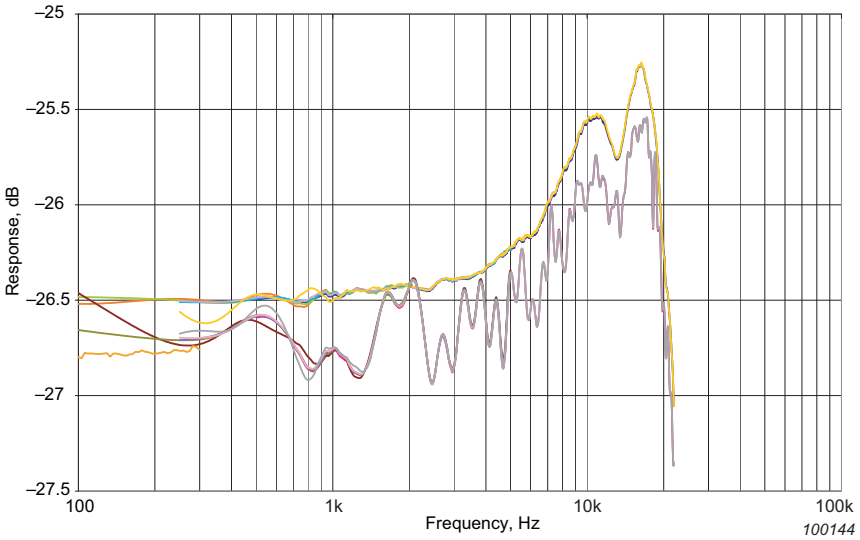

Fig. 6. 2σ of measurements carried out in widely different setups. The blue curve is for the microphone alone; the red curve is for the microphone mounted on the sound level meter. The results shown are considered valid from 200 Hz

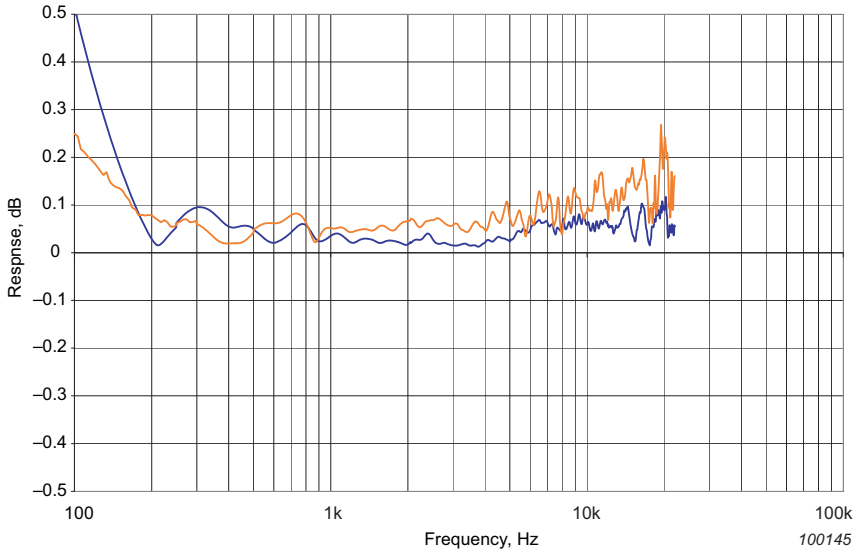

Discussion and Recommendations

The purpose of this paper is to give the reader some understanding of the TSR method and to provide guidelines and recommendations to the use of the method.

It should be mentioned that the influence of the windows in the time and frequency domains discussed here are of a general nature and exist in all time selective methods. Actually, the influence of the windows in TSR is relatively easy to understand compared to methods applying non-linear sweeps.

Our recommendations are

- Make the window as long as possible, but not longer than necessary
- Object low-frequency behaviour determines the necessary window length
- Low frequencies – go closer and increase time window
- Increasing the sweep time increases signal-to-noise ratio, not resolution
- Always try with different window sizes
- Always repeat measurements
- Large rooms are preferable, whether they are anechoic or not

- The air must be stable (easier in ordinary rooms than in anechoic chambers)
- Carefully consider the reflections and which to include in the time window

Routine measurements do not, of course, need to be verified each time.

Summary

In this paper, the Time Selective Response method has been summarized and the influence of some choices of measurement parameters and their interaction with the object response have been discussed.

The importance of the right selection of time weighting function has briefly been demonstrated. It has also briefly been demonstrated that the actual frequency range of the measurement is of small importance.

Some guidelines on how to evaluate the measurement uncertainty due to the time and frequency limitations in the measurements have also been given.

References

[1] Poletti, M. A., "*Linearly Swept Frequency Measurements, Time-Delay Spectrometry, and the Wigner Distribution*", Journal of the Audio Engineering Society, 36 (6), 1988, pp 457 – 468.

[2] Struck, C. J., Biering, C. H., "*A New Technique for Fast Response Measurements Using Linear Swept Sine Excitation*", 90th Convention of the Audio Engineering Society, New York, USA 1991, preprint 3038.

[3] PULSE™ Time Selective Response (Brüel & Kjær online documentation), Brüel & Kjær, 1995.

[4] Brüel & Kjær, Audio Analyzer Type 2012 Technical Documentation, Brüel & Kjær, BE 1119 – 13, 3 – 6 to 3 – 13, 1995 (ca.).

[5] Struck, C. J., Temme, S. F., "*Simulated Free Field Measurements*", 93rd Convention of the Audio Engineering Society, New York, USA, 1992, preprint 3397.

Measurement of Absorption Coefficient, Radiated and Absorbed Intensity on the Panels of a Vehicle Cabin using a Dual Layer Array with Integrated Position Measurement*

J. Hald, J. Mørkholt and S. Gade

Abstract

In some cases it is important to be able to measure not only the total sound intensity on a panel surface in a vehicle cabin, but also the components of that intensity due to sound radiation and due to absorption from the incident field. For example, these intensity components may be needed for calibration of energy flow models of the cabin noise. A robust method based on surface absorption coefficient measurement is presented in this paper.

Résumé

Dans certaines situations, il est important de pouvoir mesurer non seulement l'intensité acoustique totale sur un panneau de l'habitacle d'un véhicule, mais également, du fait de phénomènes de rayonnement sonore et d'absorption caractérisant le champ incident, les composantes de cette intensité. Ces composantes peuvent notamment s'avérer nécessaires pour le calibrage des modèles de flux d'énergie du bruit généré dans l'habitacle. Une méthode robuste, basée sur la mesure du coefficient d'absorption de la surface, est présentée ici.

Zusammenfassung

Manchmal ist es wichtig, dass man an einer Innenfläche in der Fahrzeugkabine nicht nur die Gesamtschallintensität misst, sondern außerdem ermitteln kann, welcher Anteil der Intensität auf Schallabstrahlung von der Fläche zurückzuführen ist und welcher auf die Absorption von Energie aus dem einfallenden Schallfeld. Diese Intensitätskomponenten werden beispielsweise zur Kalibrierung von

* First published at JSAE Annual Congress 2010, Yokohama, Japan

Energieflussmodellen des Kabinengeräuschs benötigt. Dieser Artikel stellt eine robuste Methode vor, die auf der Messung des Absorptionskoeffizienten von Flächen beruht.

Introduction

Consider the radiation of sound from a small surface segment in a cabin environment. Such a surface segment may radiate sound energy because of external forcing, causing the surface to vibrate, and it may absorb energy from an incident sound field because of finite surface acoustic impedance. When measuring the sound intensity over the surface segment with an intensity probe, the total intensity I_{tot} will be measured. Assuming the radiated field and the incident field to be mutually incoherent, the total intensity is equal to the sum of the radiated sound intensity I_{rad} that would exist with no incident field and the sound intensity component I_{abs} due to absorption from the incident field:

$$I_{\mathrm{tot}} = I_{\mathrm{rad}} + I_{\mathrm{abs}} \tag{1}$$

Considering the intensity in the outward normal direction on the panel surface, the radiated intensity will typically be positive, while the component due to absorption will typically be negative. So for vibrating panels with an absorptive surface, the total measured intensity may be small although the radiated intensity is relatively high. Often it is of interest to know not only the total intensity, but also the components due to radiation and absorption. For example, this kind of information is needed in energy-based modeling that describes the energy flow between sub-systems [1].

The method presented here is based on separation of different sound field components via the spatial sound field information provided by an array. The radiated intensity is estimated as the intensity that would exist, if the incident and scattered field components could be removed. So a free-field radiation condition is simulated. The idea is to first separate the incident field component, then use separately measured information about the scattering properties of the panel to calculate the scattered field, and finally subtract the incident and scattered fields from the total sound field. The method needs the panel geometry, which is either imported as CAD or measured with a 3D digitizer, and then uses a measured map of absorption coefficient. The separate measurement of the surface absorption coefficient is obtained using loudspeaker excitation.

Description of Methodology

The array measurements considered here are cross-spectral measurements of the full cross-spectral matrix between all array microphones and, based on that, a representation in terms of Principal Components is extracted [2]. As a consequence, no phase information is available between different array positions, so a separate processing has to be performed for each position. For each Principal Component a separate holography calculation is performed. Since these calculations are identical only one will be described. We used a Double Layer Array (DLA), and the processing was performed using Statistically Optimized NAH (SONAH) [3, 4]. A complex time harmonic representation, with the time variation $e^{j\omega t}$ suppressed, will be used.

Extraction of the Incident Field

A basic array processing task is that of extracting the incident sound field from the total sound field. However, considering the sound field on a small panel segment in a cabin, the distinction between the incident field and the radiated field is not obvious, even when we look at the field very near the panel segment. Because of coherent vibration components and significant mutual radiation impedances between neighbouring panel segments, some neighbouring segments should be included as sources of the radiated field. Fig. 1 illustrates how this distinction can be made in practice with a DLA. Using SONAH on a DLA measurement, the sound field components $(p^-, \mathbf{u}^-)$ and $(p^+, \mathbf{u}^+)$ with sources on different sides of the array plane can be separated, [3, 4]:

$$(p_{\text{total}}, \mathbf{u}_{\text{total}}) = (p^-, \mathbf{u}^-) + (p^+, \mathbf{u}^+) \tag{2}$$

The array must then be used in such a way that the pressure p^- and the velocity vector $\mathbf{u}^-$ represent the field incident on the source area of interest, while the outward propagating field component $(p^+, \mathbf{u}^+)$ is the sum of the scattered and radiated fields:

$$(p^+, \mathbf{u}^+) = (p_{\text{sct}}, \mathbf{u}_{\text{sct}}) + (p_{\text{rad}}, \mathbf{u}_{\text{rad}}) \tag{3}$$

Fig. 1a illustrates the case of an isolated source object, where the incident and outward propagating field components are well-defined. They could be determined, for example, based on measurements across two concentric spherical surfaces that enclose the test object. Microphones on the two surfaces would be

pointing to the centre, but facing in opposite directions. Fig. 1b illustrates the case of measurement on a panel section in a cabin. In this case, the measurement plane will define the distinction between sources of the incident field and sources of the outward propagating field. Here a DLA (see Fig. 3) could be used, where microphones are mounted back to back. The distinction will, however, not be sharp due to the limited angular resolution of a practical array.

*Fig. 1. Separation of inward (incident) and outward propagating field components (p^-, $\mathbf{u}^-$) and (p^+, $\mathbf{u}^+$): **a)** Clearly separated sources. **b)** Smooth transition between sources*

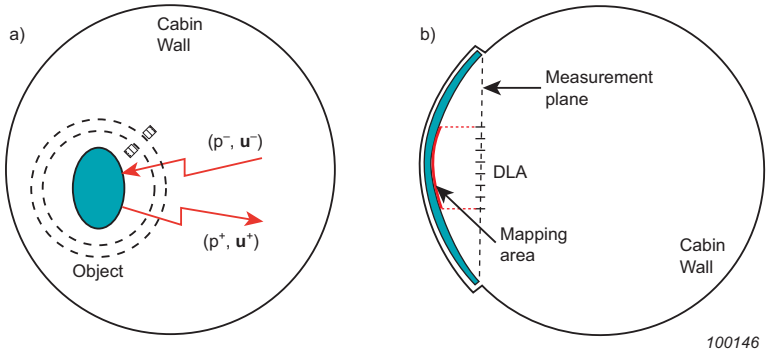

Solution of the Scattering Problem

Provided the incident and radiated fields are mutually incoherent, then Eq. (1) is the basis for a simple and robust energy based method. The basic assumption is that we can measure a local absorption coefficient α at each point $\mathbf{r}$ on the source surface such that the normal components I^- and I_{abs} of the incident and absorbed intensities are related by:

$$I_{abs}(\mathbf{r}) = \alpha(\mathbf{r})\, I^-(\mathbf{r}) \tag{4}$$

In general the ratio $I_{abs}(\mathbf{r})/I^-(\mathbf{r})$ between the two intensities will depend on the form of the incident field. If, however, the coefficient $\alpha(\mathbf{r})$ is measured with an incident field that is sufficiently similar to the incident field under operational conditions, then Eq. (4) can provide good results with the operational field.

The method requires a separate set of DLA measurements with artificial speaker excitation. Fig. 2 illustrates a setup with a set of incoherently excited speakers to create an incident field similar to the field incident under, for example, flight conditions in an aircraft. As mentioned already, the DLA/SONAH measurement

Fig. 2. Cabin panel section with surface calculation points covered by a specific array position. Speakers for measurement of surface properties are shown

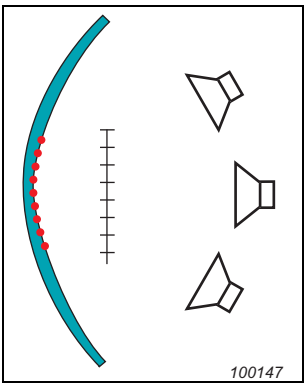

can provide the total and incident components of the loudspeaker generated sound field on the panel surface. Since in this case the absorbed intensity is equal to the total intensity, then in accordance with Eq. (4) the absorption coefficient is calculated as the ratio between the total and the incident intensities. Accurate measurement of the array positions relative to the panel geometry using an integrated position measurement system allows the absorption coefficients to be calculated at predefined points on the panel surface, see Fig. 2.

For the case of car cabin application, the surface property measurement will typically be performed with the car at a standstill, while the operational measurement will be performed during driving. Often, a single surface property measurement will be applied with several operational measurements, corresponding to different operational conditions.

Once an operational measurement has been taken, the associated total, incident and outgoing field components on the panel surface can be estimated using SONAH. The absorbed intensity is estimated using Eq. (4), and the radiated intensity is then obtained using Eq. (1).

Measurement

Measurement System

The system for data acquisition is based around the DLA shown in Fig. 3. The array has 8 × 8 microphones mounted in 2 layers, resulting in a total of 128

Fig. 3. Double-layer array (DLA) mounted with six infrared (IR) LEDs

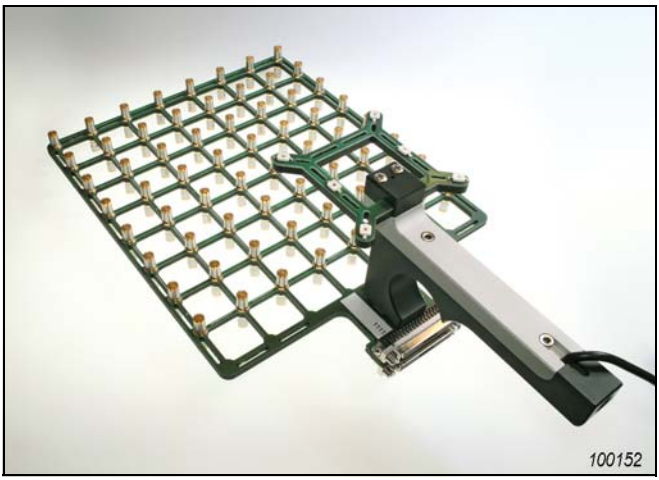

microphones. The microphones are spaced 30 mm apart in both directions and with a spacing of 31 mm between the two layers. This results in an upper frequency limit for the array of 5.7 kHz (spatial sampling limit). Also mounted on the array are six infrared LEDs, which are used in connection with a position measurement system monitoring the array position and orientation on-line. This system is based around an integrated camera unit. The camera unit has 3 built-in line cameras that determine the LED positions. The camera unit is connected to a controller box which communicates with a PC via RS−232. The LEDs on the array are also connected to this controller box. The position measurement system also has associated with it a wireless pointing device for measuring 3D point positions. This device can be used in connection with the measurement software to record 3D position data on the surfaces under investigation.

The DLA is connected to two 65-channel front-ends which are connected to the controlling PC via LAN. A third front-end with generator units is used for driving artificial excitation speakers through power amplifiers.

The controlling PC is running measurement software with a dedicated measurement template for acquisition of array microphone signals and corresponding array positions in space, as well as surface point position data. As outlined above, the analysis method requires a model of the surfaces to be analysed. Such a model can either be imported from CAD or digitized on the spot. Digitizing involves point measurements as outlined above, followed by curve and

surface construction. In both cases, the end result is a CAD-type parametric surface description which is later used as the basis for creating a surface mesh. This mesh is in turn used for calculation and results display.

Measurement Procedure

The DLA is placed in positions close to the surfaces under investigation to sample the near field sound pressure. The position of the array is recorded online via the position measurement system and microphone time histories are recorded for each array position. The array is placed in slightly overlapping positions to cover the investigated surfaces patch by patch. The data acquisition software displays the current and past array positions in 3D along with the surface model. In this way the user can identify which parts of the surface have been covered with the array and which parts still need to be covered.

When measuring for the estimation of surface absorption, a number of loudspeakers are distributed in the cabin interior and driven by uncorrelated noise sources, to create a distributed and (close-to) diffuse excitation field. Measurement for the actual estimation of entering intensity is, of course, performed in operating conditions with these sources turned off. All recorded data are stored to a database.

Data Processing

The post-processing software application retrieves all data from the database. A surface mesh is created based on the parametric surface description. A number of mesh areas may be defined in this process. These can be used for averaging of, for example, absorption coefficient.

The time histories measured in each array position are processed as shown in Fig. 4. First the full cross-spectral matrix, CSM, for all signals is calculated by FFT and the frequency responses corrected with response correction data from the individual microphones using TEDS. Then a principal component decomposition (PCD) is performed to determine the most significant incoherent components. Each component is finally processed via SONAH to determine the corresponding incoming and outgoing sound field quantities on the source surface.

From this point on, the processing depends on the quantity to be determined. The case of absorption coefficient estimation is illustrated in Fig. 5. Based on the partial sound field quantities, the total incoming and outgoing surface intensity components are calculated for surface points corresponding to each array patch. Results from different patches are then averaged on the surface mesh using a scoring method, wherein each mesh node-to-array position combination is assigned a score depending on how the node is positioned relative to the array. If

Fig. 4. Processing steps for each array position

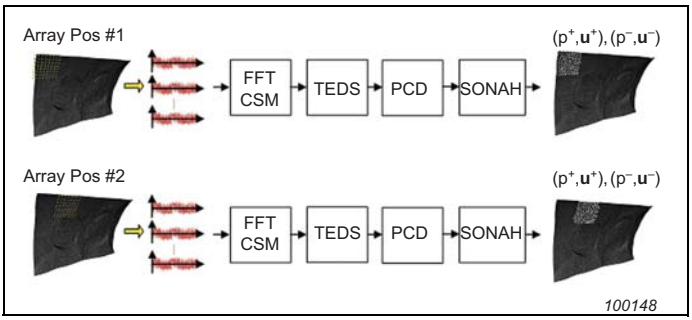

Fig. 5. Processing for absorption coefficient estimation

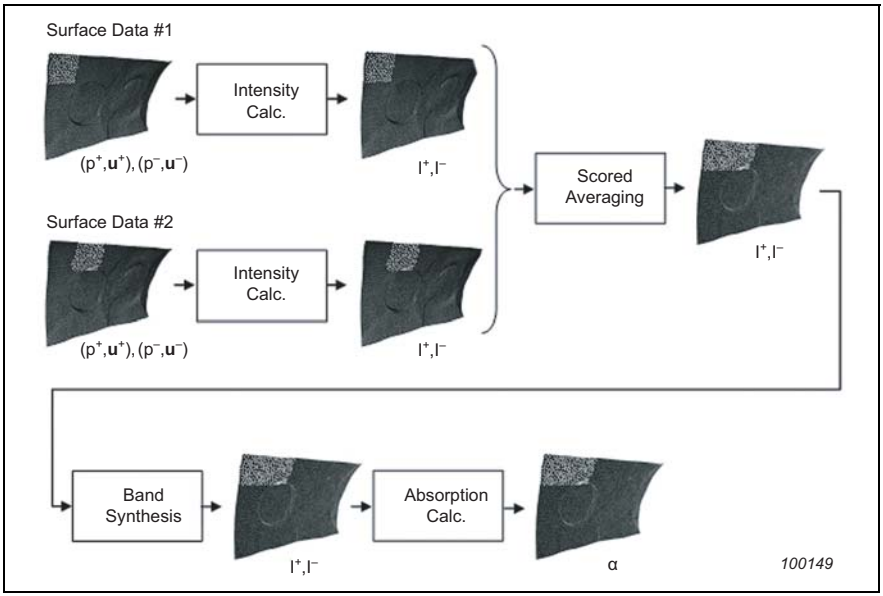

more than one array position contributes to a node, the results for that node are averaged using the scores. In this way, a contribution estimated with a "well-positioned" array will be given more weight in the averaging. The surface intensity values are then band-synthesised into, for example, 1/3-octave bands and optionally averaged over predefined averaging areas. Finally, the absorption coefficient is estimated in each node using Eq. (4).

Example: Mapping of Absorption Coefficient in a Car Cabin

To illustrate the use of the proposed techniques in an automotive application, measurements were made with the DLA system in the cabin of a Volvo S60 passenger car to determine the in-situ absorption coefficient of selected surfaces in the cabin. Firstly, the cabin surfaces to be investigated were digitized using the 3D position measurement system and dedicated digitizing software. Next, array measurements were made with the DLA covering the surfaces patch by patch. Four loudspeakers were distributed in the cabin and driven by white noise to provide the acoustic excitation needed for the estimation of the absorption coefficient.

Fig. 6. A contour plot of the estimated absorption coefficient of seat, door, window and roof in a car cabin. Results are shown for the 200 Hz 1/3-octave band. Note that results are averaged also over the respective areas

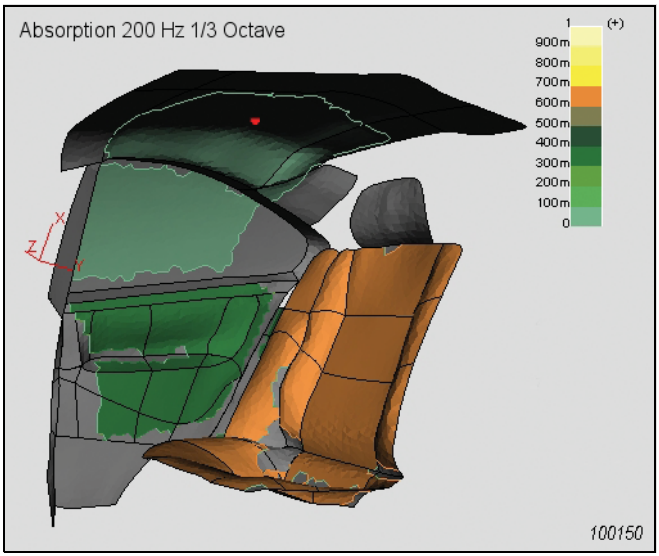

Fig. 6 shows a 3D contour plot of the estimated absorption coefficient on the cabin surfaces for the 200 Hz 1/3-octave band. The absorption coefficient was estimated by first doing 1/3-octave band synthesis of the estimated total and incident intensities, and then doing area averaging of these quantities over, for example, the seat or window surface before estimating the final absorption coefficient as the ratio between the two. The figure shows that in the 200 Hz

frequency band, the seat has quite a high absorption coefficient compared to the door, window and roof.

Fig. 7. Estimated absorption coefficient on the roof, seat and window of the car cabin as functions of frequency. Results are shown in 1/3-octave bands

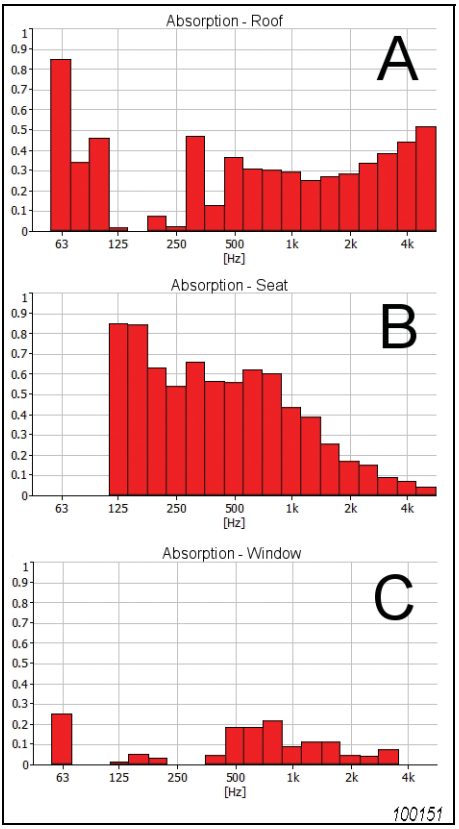

Fig. 7 shows the estimated average absorption coefficients in 1/3-octave bands for the roof (A), the seat (B) and the window (C). The roof was covered by a thin layer of foam material, which could be expected to have an absorption coefficient increasing with frequency, as the graph shows. The seat shows an absorption coefficient decreasing with frequency, which could be explained by the seat being a leather type of material that is probably acoustically "hard" at higher

frequencies. Finally, the window shows quite a low absorption coefficient throughout the whole frequency range under investigation, as could be expected.

Conclusion

A method for measuring the absorption coefficient, radiated and absorbed intensity on the panels of a vehicle cabin has been described and it was shown how the method can be used to map, for example, the absorption coefficient on the interior surfaces of a car cabin. The method is based on a Dual Layer Array with integrated position measurement. The method has shown good ability to determine the actual radiated sound intensity in the presence of a diffuse field in the cabin.

Aknowledgements

This paper is based on work done in the European Union research project Cabin noise Reduction by Experimental and numerical Design Optimization, CREDO, which deals with noise in aircraft and helicopter cabins. Since the radiated intensity is often seen from the perspective of the cabin, it is sometimes also called Entering Intensity (EI) [4]. Simulations as well as results of measurement inside aircraft can be found in [4, 7].

References

[1] Hardy, P., Trentin, D., Jézéquel, L., Ichchou, M. N., "*Identification of noise sources in an in-flight aircraft by means of local energy method*"; Proceedings of Euronoise 2006.

[2] Hald, J., "*STSF – a unique technique for scan-based Near-field Acoustical Holography without restrictions on coherence*"; Brüel & Kjær Technical Review, No. 1, 1989.

[3] Hald, J., "*Patch holography in cabin environments using a two-layer handheld array with an extended SONAH algorithm*"; Proceedings of Euronoise 2006.

[4] Hald, J., Mørkholt, J., "*Methods to estimate the Entering Intensity and their implementation using SONAH*"; Report DWP 2.3 from the European project CREDO, 2007.

[5] Alvarez, J. D., Jacobsen, F., "*In-situ measurements of the complex acoustic impedance of porous materials*"; Proceedings of Inter-Noise 2007

[6] Hald, J., Mørkholt, J., "*Array based Measurement of Radiated and Absorbed Sound Intensity Components*"; Proc. Acoustics '08, 2008

[7] Hald, J., Mørkholt, J., Hardy, P., Trentin, D., Bach-Andersen, M., Keith, G., "*Measurement of Absorption Coefficient, Surface Admittance, Radiated Intensity and Absorbed Intensity on the Panels of a Vehicle Cabin using a Dual Layer Array with Integrated Position Measurement* "; Proceedings of SAE, 2009

ISO 16063–11: Uncertainties in Primary Vibration Calibration by Laser Interferometry – Reference Planes and Transverse Motion*

Torben Licht and Sven Erik Salbøl

Abstract

Primary vibration calibration by laser interferometry using quadrature outputs has been used for the last 10 to 15 years. ISO 16063–11 [1] was published in 1999 and has increased the interest further. With the advent of new compact laser interferometers, the difficulties of optical alignment and adjustment have been practically eliminated, and dedicated software has made the process automatic, which facilitates collection of much more data.

In most cases the method is applied to reference transducers, either single-ended or those meant for back-to-back calibration. Because the laser beam cannot always be directed towards an ideal point or surface, significant errors can be introduced. At low frequencies this is often due to non-ideal exciter motions. At high frequencies it is often due to relative motion between points on apparently rigid mechanical structures, or rocking or bending motion of the combined structures. Some examples and solutions to these problems, including uncertainty calculations, will be presented in this paper.

Résumé

L'étalonnage primaire de vibrations par interférométrie laser avec sortie en quadrature est utilisé depuis une quinzaine d'années. La Norme ISO 16063–11 [1] publiée en 1999 connaît un intérêt croissant. Avec l'arrivée de nouveaux interféromètres de laser très compacts, les difficultés liées au réglage et à l'alignement optique ont été pratiquement éliminées, et des logiciels dédiés ont automatisé les procédures, facilitant l'acquisition d'une plus grande quantité de données.

* First published at IMEKO XIX World Congress: Fundamental and Applied Technology, Lisbon, Portugal

Dans la plupart des cas, cette méthode est appliquée pour les capteurs de référence, qu'ils soient accélerometre de transfert monobase ou destinés à l'étalonnage dos-à-dos. Comme le faisceau laser ne peut pas toujours être dirigé vers un point ou une surface idéal(e), des erreurs non négligeables peuvent apparaître. Aux basses fréquences, cela est souvent dû à un mouvement non idéal de l'excitateur. Aux hautes fréquences, au déplacement relatif entre points sur des structures mécaniques apparemment rigides, ou au balancement ou fléchissement de structures combinées. La présente communication exemplifie ces problèmes et leurs solutions, y compris les calculs de l'incertitude.

Zusammenfassung

Primärkalibrierung von Schwingungssensoren durch Laserinterferometrie mit Quadraturausgängen wird seit ca. 10 – 15 Jahren verwendet. Die 1999 veröffentlichte ISO 16063 – 11 [1] hat das Interesse weiter gesteigert. Mit den neuen kompakten Laserinterferometern wurden die Schwierigkeiten bei der optischen Ausrichtung und Justierung in der Praxis eliminiert. Durch Spezialsoftware wurde der Prozess automatisch gemacht, so dass sich heute wesentlich mehr Daten sammeln lassen.

In den meisten Fällen wird die Methode auf Bezugsnormalsensoren angewendet, entweder single-ended oder solche, die für Back-to-Back-Kalibrierung vorgesehen sind. Da sich der Laserstrahl nicht immer auf einen idealen Punkt oder eine ideale Fläche richten lässt, können wesentliche Fehler entstehen. Bei tiefen Frequenzen sind diese häufig auf nichtideale Bewegungen des Schwingerregers zurückzuführen, bei hohen Frequenzen dagegen auf die Relativbewegung zwischen Punkten auf scheinbar steifen mechanischen Strukturen oder auf Schaukel- oder Biegebewegungen der kombinierten Strukturen. In diesem Artikel werden einige Beispiele und Lösungen für diese Probleme vorgestellt, darunter Unsicherheitsberechnungen.

Introduction

ISO 16063 – 11, Methods for the Calibration of Vibration and Shock Transducers – Part 11: Primary Vibration Calibration by Laser Interferometry, does not go into much detail when the quality of the motion is described. The standard states:

"*Transverse, bending and rocking acceleration: Sufficiently small to prevent excessive effects on the calibration results. At large amplitudes, preferably in the*

low-frequency range from 1 Hz to 10 Hz, transverse motion of less than 1 % of the motion in the intended direction may be required; above 10 Hz to 1 kHz, a maximum of 10 % of the axial motion is permitted; above 1 kHz, a maximum of 20% of the axial motion is tolerated."

About the calibration of back-to-back accelerometers it states:

"*Typically, a 20 g mass is used. The laser light spot can be at either the top (outer surface) of the dummy mass or the top surface of the reference accelerometer.*

If the motion is sensed at the top of the dummy mass, then the dummy mass should have an optically polished top surface, and the position of the laser-light spot should be close to the geometrical centre of this surface. In cases where the motion of the mass departs from that of a rigid body, the relative motion between the top (sensed) and bottom surfaces shall be taken into consideration. To simulate a mass of 20 g of typical transfer standard accelerometers, a dummy mass in the form of a hexagonal steel bar 12 mm in length and 16 mm in width over flats of hexagonal faces can be used. At a frequency of 5 kHz, for example, the relative motion introduces systematic errors of 0.26 % in amplitude measurements and 4.2° in phase shift measurements".

The standard also states uncertainties attainable as:

"*For the magnitude of sensitivity:*

0.5 % of the measured value at reference conditions;

< 1 % of the measured value outside reference conditions."

The standard was mainly written to help national metrology institutes (and similar laboratories) to work in similar ways. These have, since the publication of the standard, claimed far better uncertainties (0.1 to 0.5 % in the full frequency range).

In these cases, the motion has normally been measured at the reference surface of the reference accelerometer, and a slotted mass has been used.

This means that the point(s) at which the motion is measured by the interferometer are positioned at a distance of some millimetres from the centre. This makes the transverse motion, which is normally a rocking motion, a major contributor to the uncertainty.

To avoid this, a dummy mass, as described above, can be used and the motion measured at the centre. However, this leaves the problem of estimating (with great accuracy) the motion at the interface between the dummy mass and the reference accelerometer.

Transverse Motion of Exciters

Manufacturers of exciters do sometimes give specifications for transverse motion, but the way these are obtained is rarely given and they are probably measured using mostly small, carefully symmetrical loads, placed directly on top of the moving element. Therefore, an investigation of actual transverse motion was performed on three different exciters. One was a classical spring controlled model, the other two were air-bearing exciters with a specified low transverse motion.

Exciters A and B are air-bearing types; exciter C is a classical spring type. Measurements on A and B were made orthogonal to the excitation direction in two different directions (X and Y, 120 degrees apart) at the top end of a reference transducer (Brüel & Kjær Type 8305), with a 20 gram slotted load-mass at the mounting surface of the accelerometer (Fig. 1). (The slotted load-mass is of PTB design and is normally used for laser interferometry, Fig. 24.) On exciter C, Type 8305 was loaded with a cubic 30 gram block with four identical accelerometers mounted on its surfaces to measure the transverse motion (Fig. 2). Measurements from two accelerometers orthogonal to each other are made use of.

Fig. 1. Slotted mass on Type 8305

Fig. 2. Cubic block on Type 8305

The results are plotted in three groups: Figs. 3 – 8 are for exciter A, Figs. 9 – 14 for exciter B, and Figs. 15 – 20 for exciter C. The excitation was a random signal and the spectrum obtained as measured by the Type 8305 is shown in the bottom left-hand graph for each of the three groups mentioned above. The transverse motions relative to the main direction for each shaker are shown as the first two curves on the left-hand side of each group. The maximum on the graphs corresponds to 100% transverse motion. From the results, it became clear that the specifications for transverse motion are not useful for estimating the motion and uncertainties related to transverse motion when a back-to-back reference transducer is mounted directly on top of the exciter table. The combined structure of the exciter table and the reference transducer shows high transverse levels in the

4 to 9 kHz range, probably due to bending modes. A small asymmetrical load (introduced by the connector) can apparently create large rocking motions, typically with peaks of 30 to 60%.

Fig. 3. Exciter A, X-direction, 8305, 20 gram

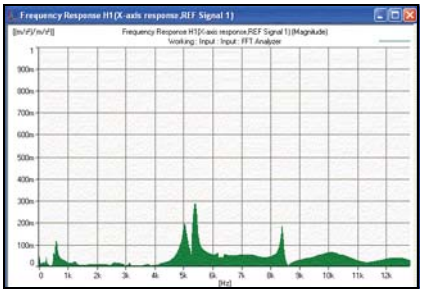

Fig. 4. Exciter A, X-direction, 8305, 20 gram, with mechanical filter

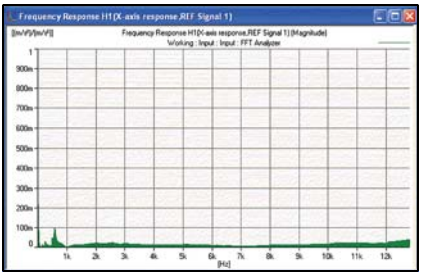

Fig. 5. Exciter A, Y-direction, 8305, 20 gram

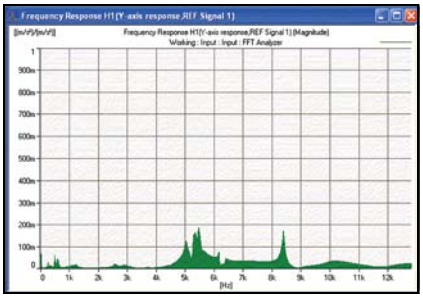

Fig. 6. Exciter A, Y-direction, 8305, 20 gram, with mechanical filter

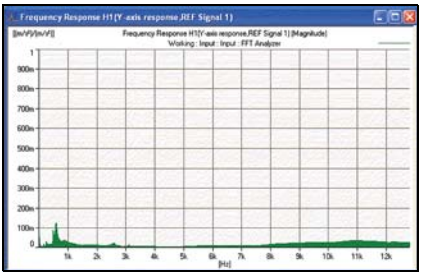

Fig. 7. Exciter A, excitation spectrum

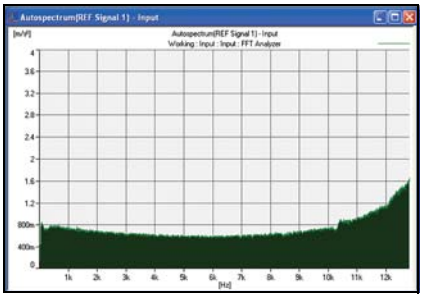

Fig. 8. Exciter A, excitation spectrum, with mechanical filter

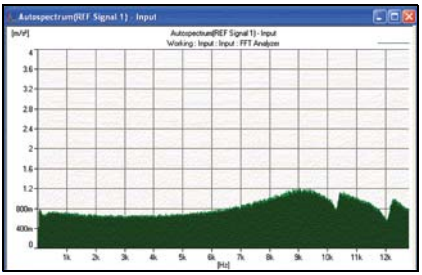

Fig. 9. Exciter B, X-direction, 8305, 20 gram

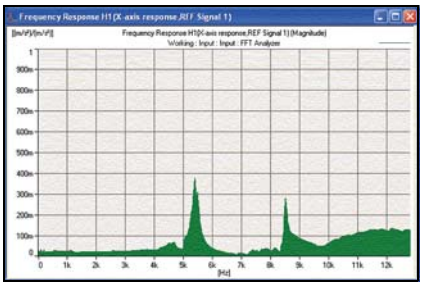

Fig. 10. Exciter B, X-direction, 8305, 20 gram, with mechanical filter

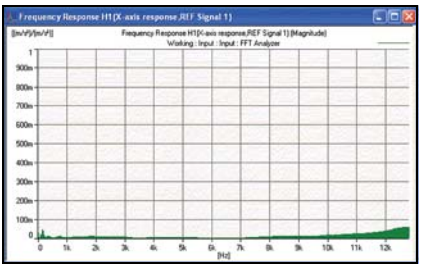

Fig. 11. Exciter B, Y-direction, 8305, 20 gram

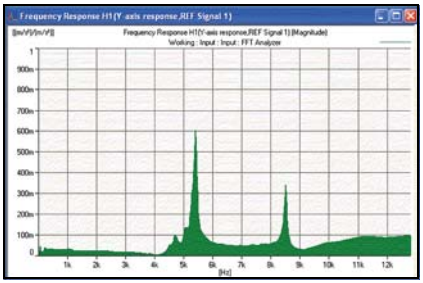

Fig. 12. Exciter B, Y-direction, 8305, 20 gram, with mechanical filter

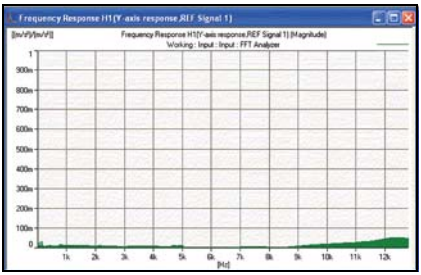

Fig. 13. Exciter B, excitation spectrum

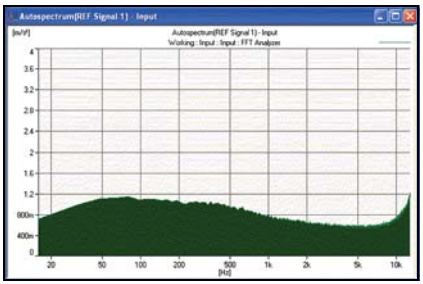

Fig. 14. Exciter B, excitation spectrum, with mechanical filter

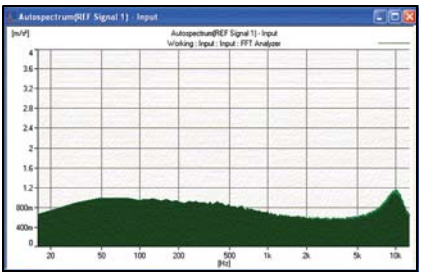

Fig. 15. Exciter C, X-direction, 8305, 20 gram

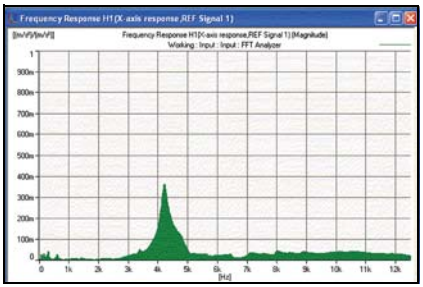

Fig. 16. Exciter C, X-direction, 8305, 20 gram, with mechanical filter

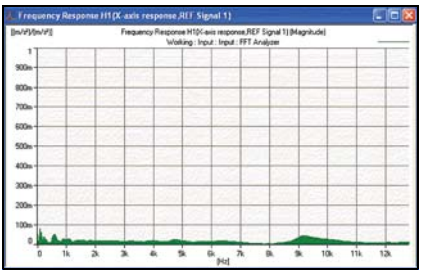

Fig. 17. Exciter C, Y-direction, 8305, 20 gram

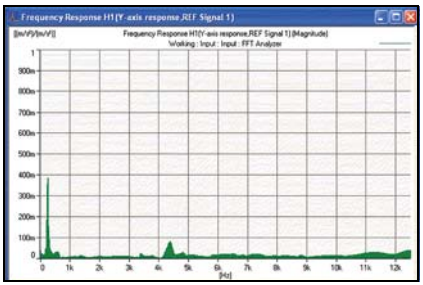

Fig. 18. Exciter C, excitation spectrum, with mechanical filter

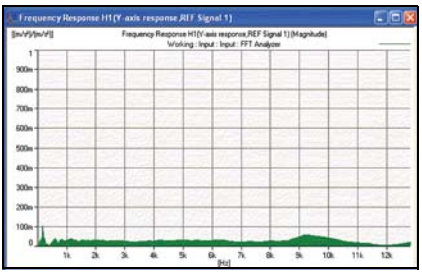

Fig. 19. Exciter C, excitation spectrum

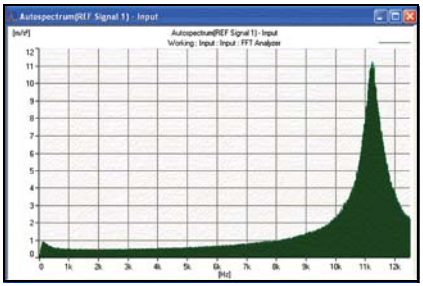

Fig. 20. Exciter C, excitation spectrum, with mechanical filter

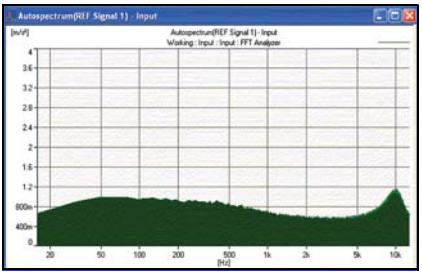

A number of experiments were performed in order to investigate this phenomenon. The best solution was found to be a mechanical filter mounted between the exciter and the reference transducer. To give the best results, the filter should be optimised (preferably) for the specific type of reference transducer. The principle of the mechanical filter is shown in Fig. 21. The filter consists of two stainless steel parts connected by vulcanized rubber.

The resulting transverse motion is now reduced to less than 5% above 1 kHz for all the exciters, as shown by the bottom right-hand graph in each of the three groups. The results from using such a filter are shown as the curves on the right-hand side of each group (Fig. 3 – Fig. 20).

Fig. 21. Cross-section of the mechanical filter

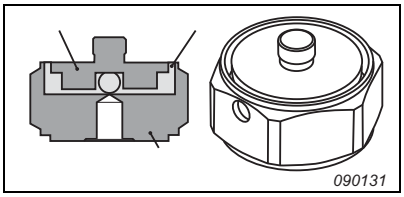

Transverse Motion Influence on Calibration Results

To avoid, or cancel out the influence of the rocking motion, the laser beam can be aligned with the centre line of the accelerometer (provided the rocking centre is also aligned on that line), or the average of two or more measurements can be made at symmetrical points about the centre line. However, rocking will always influence the measurement due to point positioning accuracy and the unknown centre line of the motion. To measure the importance of this, a series of measurements close to the critical frequencies were made. The results are shown in Fig. 22.

It can be seen that the difference between two diagonal points can be nearly ± 10%, without the filter, compared to about ±2% when the filter is used. That makes a big difference when the average has to be found. The influence can change the calculated uncertainties dramatically. If an off-centre position of 1 mm is used together with a distance to the rocking centre of 50 mm, then changing the transverse motion from 5% to 25% will increase the estimated 2σ uncertainty of 0.4% to more than 0.8%.

Fig. 22. Measurement differences with and without mechanical filter (20 gram slotted mass)

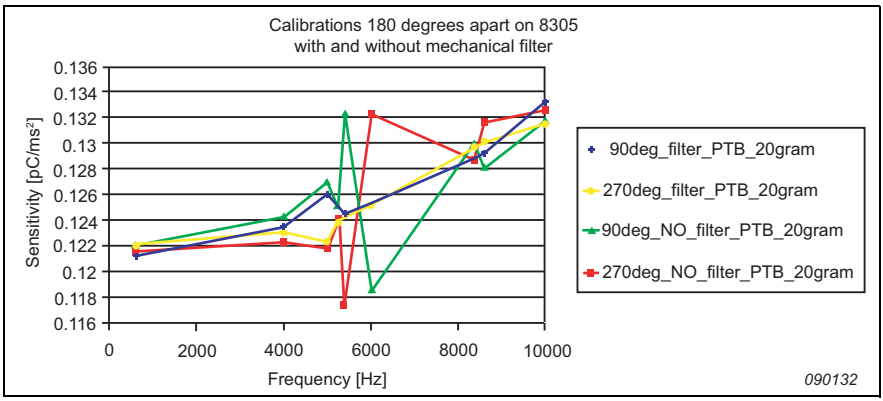

To further prove the validity of the method, a comparison was made to a well-known reference transducer in Germany, see Fig. 23.

The figure shows the result of the comparison between a calibration performed at PTB, Germany, and the calibration made at DPLA* using a mechanical filter and four points with the slotted load-mass shown in Fig. 24.

The uncertainties from the PTB certificate (0.2%, 0.3% and 0.4%) were used together with the presently stated DPLA uncertainties of 0.4% and 0.6% (above 5 kHz).

Fig. 23. E_n values comparing a recently PTB calibrated Type 8305 with a calibration at DPLA using the mechanical filter

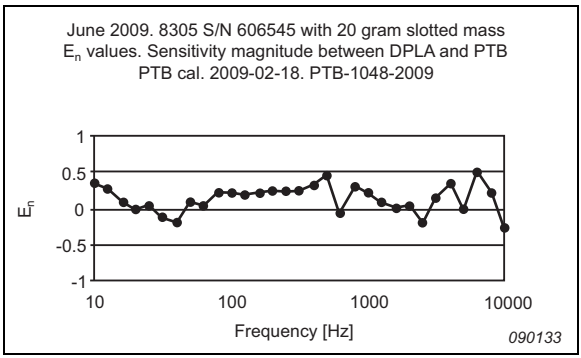

* Danish Primary Laboratory for Acoustics

Fig. 24. Stainless steel 20 gram slotted load-mass

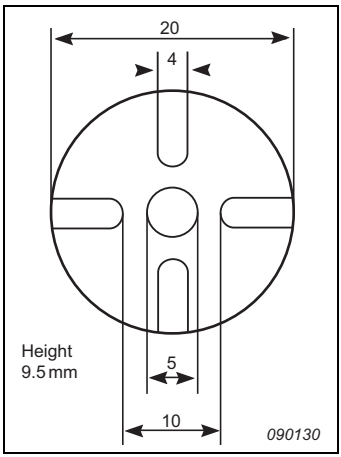

Influence of Load-Mass on Calibration Results

For the last twenty years (or more) a number of correction curves have been used for back-to-back reference transducers. Recently, some astonishing new results were published by PTB [2].

Fig. 25. Difference between measurement on top of load-mass and at the transducer surface

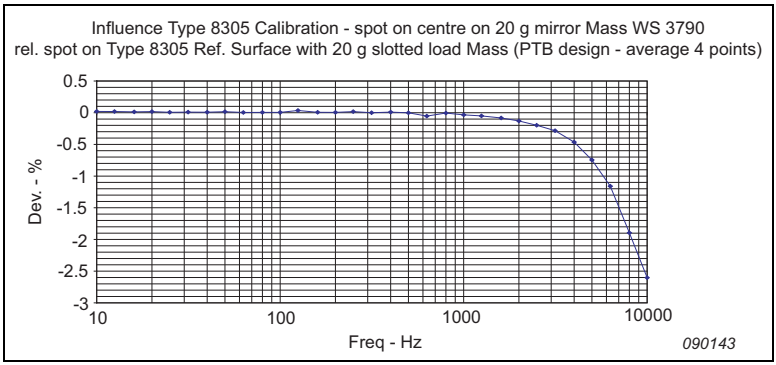

At DPLA a number of measurements were undertaken to question and verify these new results. One of the first measurements was to compare the results on top of a 20 gram solid stainless steel mass (as described in the standard [1]), to the results obtained at the interface between the transducer and a slotted 20 gram mass. The difference is shown in Fig. 25, and this shows a deviation well beyond the value stated in the standard.

A number of measurements similar to the results reported in [2] are in the process of being completed, but these seem to confirm the findings.

Conclusions

The transverse motion of different shakers has been investigated. The results show that even high quality shakers designed for calibration show very high levels of transverse motion at higher frequencies, when back-to-back accelerometers with load-masses are mounted on them. This is detrimental to the laser-interferometric measurements used to give the best possible primary calibrations.

A solution to this problem has been devised in the form of mechanical filters, which modify the assembly to remove the high frequency bending modes of the shaker plus accelerometer structure.

The use of slotted load-masses for calibration of back-to-back accelerometers has been taken up, and it has been shown that the difference between this and the often used mirror-masses is much larger than normally expected. This is the subject of further work and discussion.

References

[1] ISO 16063–11, "*Methods for the Calibration of Vibration and Shock Transducers – Part 11: Primary Vibration Calibration by Laser Interferometry*", 1999.

[2] Täubner, A., Schlaak, H-J., Bruns, T., "*Metrological and Theoretical Investigations of the Influence of Mass Loads on the Transmission Coefficient of Acceleration Transducers of the Back-to-back Type*", Physikalisch Technische Bundesanstalt, 38116 Braunschweig, Germany.

Previously issued numbers of Brüel & Kjær Technical Review

1 – 2009 Use of Volume Velocity Sound Sources in the Measurement of Acoustic Frequency Response Functions
Turnkey Free-field Reciprocity System for Primary Microphone Calibration

1 – 2008 ISO 16063–11: Primary Vibration Calibration by Laser Interferometry: Evaluation of Sine Approximation Realised by FFT
Infrasound Calibration of Measurement Microphones
Improved Temperature Specifications for Transducers with Built-in Electronics

1 – 2007 Measurement of Normal Incidence Transmission Loss and Other Acoustical Properties of Materials Placed in a Standing Wave Tube

1 – 2006 Dyn-X Technology: 160 dB in One Input Range
Order Tracking in Vibro-acoustic Measurements: A Novel Approach Eliminating the Tacho Probe
Comparison of Acoustic Holography Methods for Surface Velocity Determination on a Vibrating Panel

1 – 2005 Acoustical Solutions in the Design of a Measurement Microphone for Surface Mounting
Combined NAH and Beamforming Using the Same Array
Patch Near-field Acoustical Holography Using a New Statistically Optimal Method

1 – 2004 Beamforming

1 – 2002 A New Design Principle for Triaxial Piezoelectric Accelerometers
Use of FE Models in the Optimisation of Accelerometer Designs
System for Measurement of Microphone Distortion and Linearity from Medium to Very High Levels

1 – 2001 The Influence of Environmental Conditions on the Pressure Sensitivity of Measurement Microphones
Reduction of Heat Conduction Error in Microphone Pressure Reciprocity Calibration
Frequency Response for Measurement Microphones – a Question of Confidence
Measurement of Microphone Random-incidence and Pressure-field Responses and Determination of their Uncertainties

1 – 2000 Non-stationary STSF

1 – 1999 Characteristics of the Vold-Kalman Order Tracking Filter

1 – 1998 Danish Primary Laboratory of Acoustics (DPLA) as Part of the National Metrology Organisation
Pressure Reciprocity Calibration – Instrumentation, Results and Uncertainty
MP.EXE, a Calculation Program for Pressure Reciprocity Calibration of Microphones

(Continued on cover page 3)

www.bksv.com

BV 0062 – 11 ISSN 0007 – 2621

HEADQUARTERS: Brüel & Kjær Sound & Vibration Measurement A/S
DK-2850 Nærum Denmark · Telephone: +45 7741 2000 · Fax: +45 4580 1405
www.bksv.com · info@bksv.com

Local representatives and service organisations worldwide

Brüel & Kjær

creating sustainable value